AIP | Applied Physics Letters

Graphene grown out of diamond

Changzhi Gu, Wuxia Li, Jing Xu, Shicong Xu, Chao Lu, Lifang Xu, Junjie Li, and Shengbai Zhang

Citation: Applied Physics Letters **109**, 162105 (2016); doi: 10.1063/1.4964710
View online: http://dx.doi.org/10.1063/1.4964710
View Table of Contents: http://scitation.aip.org/content/aip/journal/apl/109/16?ver=pdfcov
Published by the AIP Publishing

Graphene grown out of diamond

Changzhi Gu,[1,2,3,a)] Wuxia Li,[1,a)] Jing Xu,[4] Shicong Xu,[1] Chao Lu,[1] Lifang Xu,[1] Junjie Li,[1] and Shengbai Zhang[5]
[1]*Beijing National Laboratory for Condensed Matter Physics, Institute of Physics, Chinese Academy of Sciences, Beijing 100190, China*
[2]*Collaborative Innovation Center of Quantum Matter, Beijing, China*
[3]*School of Physical Sciences, CAS Key Laboratory of Vacuum Physics, University of Chinese Academy of Sciences, Beijing 100190, China*
[4]*Department of Physics, Renmin University of China, Beijing 100872, China*
[5]*Department of Physics, Applied Physics, and Astronomy, Rensselaer Polytechnic Institute, Troy, New York 12180, USA*

(Received 13 July 2016; accepted 28 September 2016; published online 19 October 2016)

Most applications of graphene need a suitable support substrate to present its excellent properties. But transferring graphene onto insulators or growing graphene on foreign substrates could cause properties diminishing. This paper reports the graphene growth directly out of diamond (111) by B doping, guided by first-principles calculations. The spontaneous graphene formation occurred due to the reconstruction of the diamond surface when the B doping density and profile are adequate. The resulting materials are defect free with high phase purity/carrier mobility, controllable layer number, and good uniformity, which can be potentially used directly for device fabrication, e.g., high-performance devices requiring good thermal conductivity. *Published by AIP Publishing.* [http://dx.doi.org/10.1063/1.4964710]

Graphene is a single-atomic-layer material with fascinating physical and chemical properties such as the anomalous quantum Hall effect, minimal conductance at zero gate voltage, extraordinary mechanical strength, high thermal conductivity, and a unique ballistic transport. These make graphene an ideal material for applications in electronics, energy, information, biology, and many more fields.[1–7] Graphene was first obtained by micromechanical cleavage of graphite.[8] In most applications, it is desirable that the graphene is supported by a substrate. Growing or transferring graphene on a suitable foreign substrate while protecting its unique physical properties is, however, a daunting challenge. For example, transferring a graphene sheet onto a SiO_2 substrate has obvious disadvantages, as the properties of the graphene will be diminished by the large number of traps and consequent phonon scattering at the interface.[9–11] Therefore, it is urgent to find a substrate, for either transfer or growth, upon which graphene's crystal quality and symmetry can be preserved perfectly.

To date, various types of substrates have been used for graphene growth, including carbides, e.g., SiC, TiC, and TaC.[12,13] The high temperature thermal decomposition of carbides for graphene fabrication is, however, not compatible with current semiconductor technology and can easily produce graphene with defects. A metal substrate such as Pt, Ni, Ru, Ir, or Co is another alternative. The major drawback of the metal substrate is the strong metal-graphene interaction, which limits the size, alters the transport properties, and makes it harder to design and fabricate devices.

Diamond is a natural candidate for the dielectric substrate of graphene devices, due to its excellent physical and chemical properties such as unparalleled hardness, extremely high thermal conductivity, high hole and electron mobility, and chemical inertness. Moreover, heavily boron doped diamond is a superconductor with exceptionally high T_C for an elemental solid in ambient conditions. Both synthesized and natural industry-grade diamonds are readily and cheaply available now. Recently, improved properties of devices composed of graphene on diamond or diamond-like carbon substrate have been demonstrated, outperforming graphene on SiO_2.[11,14,15] However, in these experiments, the graphene was transferred onto a diamond surface, which generally requires surfaces of low roughness (<1 nm). The usual disadvantages of graphene transfer are also unavoidable. So the directly growing graphene on diamond is one even dream about it in this field. Several experiments have shown that one could convert nano-diamond clusters into nano-graphene islands.[16] For diamond with a (111) surface, first-principles calculations further suggested that impurity doping can cause single-layer graphitization on the surface.[16] Surface reconstruction of the diamond is the reason for the graphitization of the outermost layer(s). Very recently, a process based on rapid thermal annealing of ultra-nano-crystalline diamond in the presence of a metal catalyst was developed for the growth of high quality single and multilayer graphene into wafer scales towards the realization of graphene/diamond-based electronics without transferring of graphene onto other substrates.[17]

In this paper, we show that graphene can be grown directly out of diamond, guided by first-principles calculations. Our density functional theory calculations for boron doped diamond (111) suggest that B doping induces a configuration change of carbon on the diamond surface to sp^2 hybridization. When the doping density and profile are adequate, surface reconstruction of the diamond can lead to spontaneous formation of graphene, bound to the substrate via only weak van der Waals interactions. Our experimental results indicate that we have synthesized high-quality

[a)]Authors to whom correspondence should be addressed. Electronic addresses: czgu@aphy.iphy.ac.cn and liwuxia@aphy.iphy.ac.cn

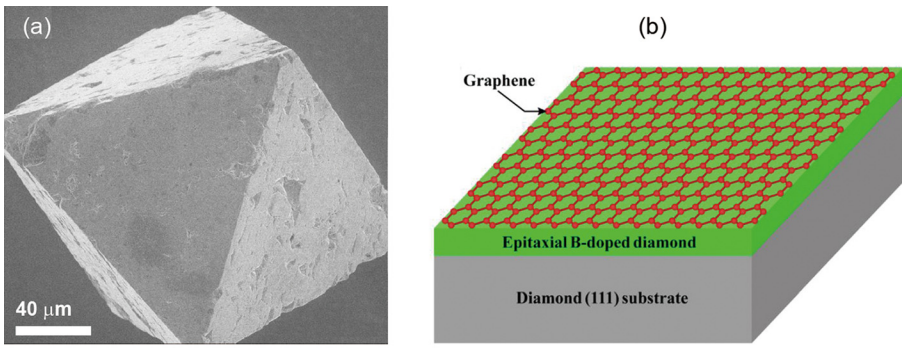

FIG. 1. (a) SEM image of the diamond (111) substrate. (b) Schematic of graphene grown out of the diamond (111) surface.

monolayer, bilayer, and multilayer graphenes on the diamond (111) surface by the B-doping. The graphene thickness can be accurately controlled by regulating the growth time. Raman study indicates that the graphenes are defect free, judging by the complete absence of the D band in the Raman spectrum. The 2D band intensities relative to the G band further indicate the good quality of the graphene layers. The mobility of the graphene layers has been estimated to be in the range of $10\,000\,cm^2/V\,s$ from the Hall measurement. These values from our untreated samples are comparable to those of untreated free-standing graphene sheets.

Unpolished single-crystal diamond (111) particles synthesized by high pressure and high temperature (HPHT) were used as the substrates. A boron doped diamond film was grown epitaxially by using a hot-filament CVD (HFCVD) method on the single crystal (SC) diamond (111) substrate. HFCVD is a standard process for growing diamond films. More details about the HFCVD system are given elsewhere.[18] Before the deposition of the diamond film, the diamond (111) substrates were ultrasonically pretreated in an ethanol solution. In addition to the CH_4 (4 sccm) and H_2 (100 sccm) used as reaction gases, boron was introduced during the growth process by bubbling H_2 gas (3–5 sccm) through a $B(OCH_3)_3$ liquid precursor at room temperature. The total pressure was at 40–55 Torr. The substrate temperature was about 700–900 °C, measured by a thermocouple mounted on the substrate. The duration of the deposition was 2–3 h, and an epitaxial B-doped diamond coating about 2 μm thick was formed. The film resistivity and carrier concentration were measured in a Bio-Rad Microscience HL5500 Hall system by the van der Pauw and Hall Effect method. Silver paint contacts were applied at the corners of the rectangular samples. The phase purity of the coatings on the diamond (111) was characterized by JY-6000 micro-Raman spectroscopy with a 532-nm laser.

Figure 1(a) shows the SEM image of the triangular (111) facet of a 200-μm diamond, and an epitaxial B-doped diamond coating covered by monolayer graphene is shown in Fig. 1(b). We used Raman spectroscopy to verify the nature of the coating. Figure 2 shows the Raman spectra of the diamond (111) substrate before and after the deposition of the B-doped diamond film. For the diamond (111) substrate, one can see clearly a strong $1332\,cm^{-1}$ peak, corresponding to optical vibration in the diamond crystal. The intensity and width of the peak confirm that the sample is a single crystal. For the diamond (111) substrate after deposition, Fig. 2(b) shows dramatically a single layer graphene on the substrate after 2 h growth. Its G peak at $1584\,cm^{-1}$ that corresponds to the E_{2g} phonon at the center of the Brillouin zone and the 2D peak at $2668\,cm^{-1}$ are also strong and clear. The major fingerprint of graphene in Raman spectra is the 2D peak; its shape, position, and intensity relative to the G peak depend sensitively on the number of layers. Figures 2(c) and 2(d) show the bilayer and multilayer graphene after 2.5 h and 3 h growth, respectively. The positions of the G and 2D peaks with respect to the ones in Fig. 2(b) have not changed at all. Note that there is no defect-related D peak in any of the examples. We know that the D peak at $1360\,cm^{-1}$ is due to the out-of-plane breathing mode of sp^2 carbon atoms and is active in the presence of defects. The D band is an effective probe to assess the level of defects and impurities in graphene; for example, it is completely absent in high-quality graphene such as the micromechanically exfoliated ones, except in the proximity of edges. On the other hand, the penetration depth of the Raman laser at 532 nm is several hundred nanometers, so the Raman signal was generated from the entire film thickness. However, in our experiment, the strong Raman signal from the diamond substrate does not appear to overshadow the expected G peak of the graphene, which can be attributed to the perfect symmetry and high quality of the defect-free graphene on the diamond (111) substrate.[19]

The low thermal boundary resistance (R_B) between the graphene and the substrate is important for applications in thermal interface materials and as a heat spreader in devices.[20] However, graphene's thermal coupling to substrate materials depends sensitively on the substrate's surface roughness and the presence of any suspended regions in the graphene layers. To transfer graphene onto a diamond, it is

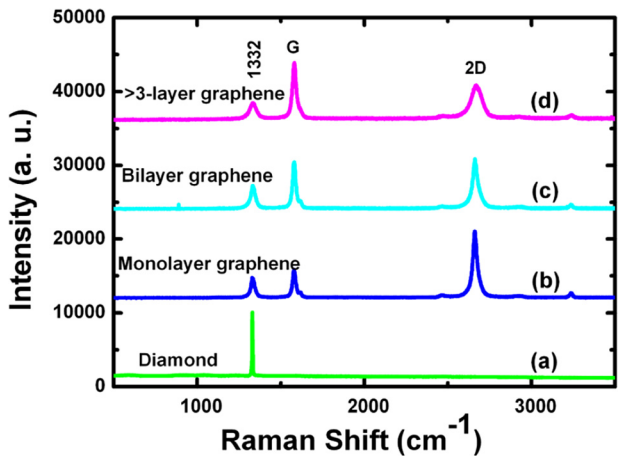

FIG. 2. Raman spectra of a diamond (111) substrate, (a) bare, and with (b) single-layer, (c) bilayer, and (d) multilayer graphene on the surface.

necessary to polish the diamond to obtain roughness of less than 1 nm.[12] However, polishing a diamond is difficult due to its hardness and hence is impractical for device applications. In our study, unpolished HPHT diamond (111) was used as the substrate, despite the surface roughness being larger than 100 nm, as can be seen in Fig. 1. Raman spectra from different regions on the (111) surface of the 200 μm diamond grain indicate the uniformity of the bilayer graphene, as shown in Fig. 3. No significant defect D peak was detected across the whole (111) facet. These results strongly suggest that growing graphene directly out of diamond (111) eliminates the substrate contact effect; thereby, the degradation of thermal conductivity that was generally found in transferred graphene on the substrate is prevented. This is important for heat dissipation in device applications.

One of the interested intrinsic properties of graphene is the high carrier mobility. At ambient conditions, the mobility in graphene on the substrate is typically on the order of several thousand $cm^2/V\,s$ (about 2000 $cm^2/V\,s$ on SiC substrate) due to surface adsorbates.[21] Improved sample preparation, including post-fabrication desorption of surface adsorbates by current annealing, enables mobility exceeding 20 000 $cm^2/V\,s$.[22] Generally, the dominant scattering mechanism of the carrier transport in graphene is due to defects. In oxide-supported graphene, trapped charges are the dominant scatterers. Because our graphene sample is grown out of its diamond substrate, it is defect-free and tends not to trap charges due to the inherent high carrier mobility of diamond (10^5–10^7 higher than that of SiO_2),[23] so the graphene layer is expected to have higher mobility here than on other substrates. However, since our graphene is grown by B doping, the graphene's mobility cannot be simply measured directly, as any possible effect of the B-doped diamond layer under the graphene must be considered.

We measured the room-temperature Hall Effect and resistivity in bilayer graphene on diamond (111). The measured resistivity is $1.6 \times 10^{-6}\ \Omega\,cm$, very close to the known resistivity of suspended graphene. The measured hole Hall mobility is 57.4 $cm^2/V\,s$. Note that the mobility here has contributions from both the graphene and the underlying B-doped diamond layer. In order to extract the mobility of the graphene, we used a parallel bilayer conductivity model where the first layer is the graphene and the second layer is the highly conductive B-doped diamond, which is 2 μm thick.[24] The Hall mobility μ_H (57.4 $cm^2/V\,s$) for the bilayer can be expressed as[24]

$$\mu_H = \frac{{\mu_{H1}}^2 n_{H1} d_1 + {\mu_{H2}}^2 n_{H2} d_2}{\mu_{H1} n_{H1} d_1 + \mu_{H2} n_{H2} d_2}, \tag{1}$$

where μ_{H1}, n_{H1}, d_1 are the Hall mobility, carrier concentration ($10^{12}\,cm^{-2}$), and thickness (0.335 nm) of the graphene layer, and μ_{H2}, n_{H2}, d_2 are the Hall mobility (10.1 $cm^2/V\,s$), carrier concentration ($1.2 \times 10^{23}\,cm^{-3}$), and thickness of the B-doped diamond coating (2 μm). To find the mobility of the substrate, we first removed the graphene by boiling the sample in $HClO_4$ and then measured the resistivity and hole mobility of the B-doped layer.

Using Eq. (1), the graphene mobility is estimated to be 1.0767×10^4 $cm^2/V\,s$. Note that our measurement was carried out in air in ambient conditions, under which the graphene easily adsorbs gaseous molecules and other contaminants from the air. Therefore, our estimated mobility should be smaller than the actual mobility of epitaxial graphene. Even so, the value of 1.0767×10^4 $cm^2/V\,s$ is still higher than in most reports of unsuspended graphene, hinting at some success here in obtaining high-quality as-grown graphene from diamond, which offers a different direction toward the important goal of minimizing the interface resistance while improving carrier mobility in graphene devices.

As mentioned earlier, first-principles calculations have been carried out to predict the growth of graphene out of diamond (111). The calculations used the Vienna *ab initio* simulation package (VASP).[25] The electron-core interactions were described by the Vanderbilt ultrasoft pseudopotential. The exchange correlation energy was described employing the generalized gradient approximation (GGA).[26] A plane wave basis set was used with a kinetic energy cutoff of 350 eV. The theoretical bulk lattice constant of diamond (3.574 Å) was used in all calculations of the diamond (111) surface. A $2 \times 2 \times 1$ k-point mesh in the Monkhorst-Pack scheme was used for Brillouin zone integration.[27] All atoms were fully relaxed except for those at the bottom two layers, which were fixed at their respective bulk positions. To minimize interactions between the top and bottom surfaces, 12 layers of carbon atoms with a bottom layer passivated by hydrogen and a vacuum region larger than 15 Å were used.

To elucidate the underlying physics for the growth of graphene on diamond, here we highlight the key findings of the first-principles calculations, while the details of the calculations and discussions will be published elsewhere. The ability to convert a surface diamond (111) bilayer into a graphene layer depends on the depth of the B dopant. If it is too deep, one can expect that the effect will be vanishingly small. The outmost surface layer may not be the best choice, either. Instead, we found that the 5th layer has low substitution energy for B, as well as being most effective in promoting surface graphitization.

Consider first the case with 1/16 B doping in the 5th layer (calculated using a 4×4 surface cell, and B is shown in pink in Fig. 4(a), whereas all other layers are free of B).

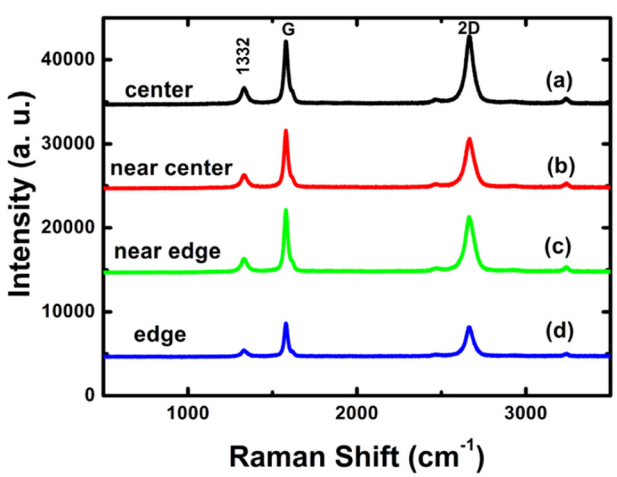

FIG. 3. Raman spectra in different regions of a 200 μm diamond (111) substrate: (a) center, (b) near center, 30 μm from center, (c) near edge, 70 μm from center, and (d) at edge, 100 μm from center.

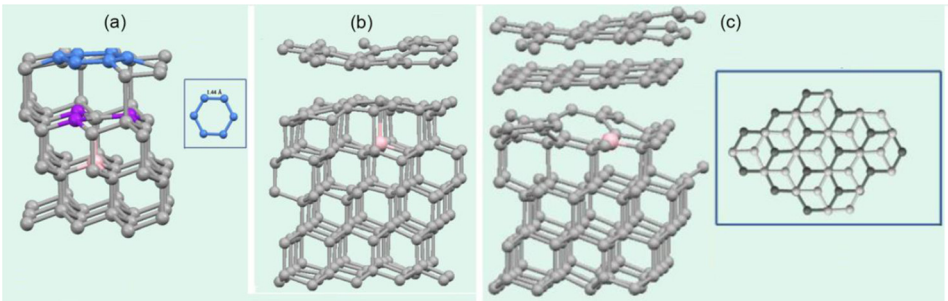

FIG. 4. (a) Optimized atomic structure at 0 K. This shows the transition of the first bilayer above the B atoms into a local hexagonal graphene-like structure (see the blue balls representing the sp^2 surface carbon). (b) Structure obtained by MD simulations when heating up the system to 900 K. (c) The structure after another 130 fs equilibration at 900 K. The inset is the top view of two layers of formed graphene. Pink ball is B and green balls are the back surface H.

Figure 4(a) shows the optimized structure at 0 K, in which a local graphene-like structure, due to bulging up of the carbon atoms in the 2nd layer (denoted by blue balls), is visible. The carbon bond lengths inside the graphene-like structure are approximately 1.44 Å instead of 1.55 Å. The distances between the carbon atoms in the 3rd layer and those in the graphene-like structure are elongated from 1.55 Å to 2.42 Å. This, compared to the normal C-C bond length 1.55 Å in bulk diamond, suggests that no more bonding exists between the carbon atoms in adjacent layers. This particular case demonstrates that shallow dopant B will induce a local sp^2 structure on the surface. Going further, we increased the B doping concentration in the 5th layer to ¼. In this case, graphene will spontaneously form even at T = 0 K, with no energy barrier.

To understand the physics of graphene forming on diamond (111) by B doping under our experimental conditions, we also performed *ab initio* molecular dynamics (MD) simulations with a time step = 0.5 fs and canonical NVT ensemble, in which we heated the system steadily to the experimental temperature, around 900 K, and a Nosé-Hoover thermostat was used to control the temperature. All atoms were allowed to move. Equilibration was reached by gradually heating the system up from 0 to 900 K. We then examined the effect of thermal oscillation on the atomic structure at around 900 K. Figure 4(b) shows that the 1st bilayer has completely become graphene. Figure 4(c) shows that when the constant-temperature dynamics continues for another 130 fs, the 2nd bilayer (i.e., atomic layers #3 and 4) also transforms to graphene. It is worth noting that the thermal effects are small in the simulation. Consider, for example, the H is used to terminate the back surface. At the end of the simulation, they all remained at their original positions. This means that thermal energy is not enough to cause structural change, not even to lift H off the back surface, despite H having only a single bond.

The physics of B inducing spontaneous formation of graphene can be summarized as follows: once a B atom is incorporated into the 5th layer, it creates a dangling bond on the nearest C atom (which in our case is in the 4th layer, right on top of the B atom). Changing the carbon from sp^3 hybridization to sp^2 hybridization, accompanied by atomic reconstruction, can reduce or eliminate the number of dangling bonds, lowering system energy. Therefore, surface reconstruction, as a result of the B doping, creates a graphene-like seed structure, which then catalyzes the growth of a larger graphene sheet. As the B concentration increases, such carbon sp^2-hybridization seeds on the surface will increase as well. Thermo fluctuation will accelerate the process where all C atoms tend toward the sp^2 state, eventually forming graphene. So the graphene formed spontaneously grows out of diamond (111) and copies the perfect symmetry of the diamond (111) surface, which presents unique properties of no defects, no suspended regions, excellent uniformity, and high carrier mobility.

In summary, we theoretically predicted and experimentally demonstrated that graphene can spontaneously form on the diamond (111) surface after B doping. This allows one to obtain the intrinsic properties of graphene on a foreign substrate, with superb characteristics of both graphene and diamond. We also found that the graphene grown this way is defect-free, with high phase purity and carrier mobility, has a controllable number of layers and good uniformity at a large scale of hundreds of microns, which might be a potential approach for fabrication of future high-performance devices based on graphene/semiconductor hetero-structures.

This work was supported by the National Natural Science Foundation of China under Grant Nos. 51272278, 61390503, 91323304, 11574369, and 11574368; XDB07020200, MOST under Grant No. 2016YFA0200402, Nanosciences Foundation in Grenoble and French ANR PNANO Project "Nanosim-Graphene" and the U.S. Department of Energy under Grant No. DE-SC0002623.

[1]J. T. Wang, H. M. Weng, S. N. Nie, Z. Fang, Y. Kawazoe, and C. F. Chen, Phys. Rev. Lett. **116**, 195501 (2016).
[2]Z. G. Chen, Z. Shi, W. Yang, X. Lu, Y. Lai, H. Yan, F. Wang, G. Zhang, and Z. Li, Nat. Commun. **5**, 4461 (2014).
[3]Z. Shi, C. Jin, W. Yang, L. Ju, J. Horng, X. Lu, H. A. Bechtel, M. C. Martin, D. Fu, J. Wu, K. Watanabe, T. Taniguchi, Y. B. Zhang, X. Bai, E. Wang, G. Zhang, and F. Wang, Nat. Phys. **10**, 743 (2014).
[4]Y. C. Tian, H. Tian, Y. L. Wu, L. L. Zhu, L. Q. Tao, W. Zhang, Y. Shu, D. Xie, Y. Yang, Z. Y. Wei, X. H. Lu, T. L. Ren, S. C. Khih, and J. M. Zhao, Sci. Rep. **5**, 10582 (2015).
[5]N. Tombros, C. Jozsa, M. Popinciuc, H. T. Jonkman, and B. J. van Wees, Nature **448**, 571–574 (2007).
[6]A. Bostwick, F. Speck, T. Seyller, K. Horn, M. Polini, R. Asgari, A. H. MacDonald, and E. Rotenberg, Science **328**, 999–1002 (2010).
[7]H. X. Yang, M. Chshiev, X. Waintal, and S. Roche, Phys. Rev. Lett. **110**, 046603 (2013).
[8]K. S. Novoselov, A. K. Geim, S. V. Morozov, D. Jiang, Y. Zhang, S. V. Dubonos, I. V. Grigorieva, and A. A. Firsov, Science **306**, 666–669 (2004).
[9]Y. M. Lin, C. Dimitrakopoulos, K. A. Jenkins, D. B. Farmer, H. Y. Chiu, A. Grill, and P. Avouris, Science **327**, 662 (2010).

[10]L. Liao, Y. C. Lin, M. Q. Bao, R. Cheng, J. W. Bai, Y. Liu, Y. Q. Qu, K. L. Wang, Y. Huang, and X. F. Duan, Nature **467**, 305–308 (2010).
[11]Y. Q. Wu, Y. M. Lin, A. A. Bol, K. A. Jenkins, F. N. Xia, D. B. Farmer, Y. Zhu, and P. Avouris, Nature **472**, 74–78 (2011).
[12]C. Soldano, A. Mahmood, and E. Dujardin, Carbon **48**, 2127–2150 (2010).
[13]F. Parvizi, D. Teweldebrhan, S. Ghosh, I. Calizo, A. A. Balandin, H. Zhu, and R. Abbaschian, Micro Nano Lett. **3**, 29–34 (2008).
[14]J. Yu, G. X. Liu, A. V. Sumant, V. Goyal, and A. A. Balandin, Nano Lett. **12**, 1603–1608 (2012).
[15]F. Zhao, A. Vrajitoarea, Q. Jiang, X. Y. Han, A. Chaudhary, J. O. Welch, and R. B. Jackman, Sci. Rep. **5**, 13771 (2015).
[16]Y. Yan, S. B. Zhang, and M. M. Al-Jassim, Phys. Rev. B **66**, 201401 (2002).
[17]D. Berman, S. A. Deshmukh, B. Narayanan, S. K. R. S. Sankaranarayanan, Z. Yan, A. A. Balandin, A. Zinovev, D. Rosenmann, and A. V. Sumant, Nat. Commun. **7**, 12099 (2016).
[18]C. Z. Gu, Y. Sun, Y. Sun, and Z. S. Jin, Diamond Relat. Mater. **11**, 405–407 (2002).
[19]L. M. Malard, M. A. Pimenta, G. Dresselhaus, and M. S. Dresselhaus, Phys. Rep. **473**, 51–87 (2009).
[20]A. A. Balandin, Nat. Mater. **10**, 569–581 (2011).
[21]K. Konishi and K. Yoh, Physica E **42**, 2792–2795 (2010).
[22]N. Tombros, A. Veligura, J. Junesch, J. J. van den Berg, and P. J. Zomer, J. Appl. Phys. **109**, 093702 (2011).
[23]Z. L. Wang, Q. Luo, L. W. Liu, C. Y. Li, H. X. Yang, H. F. Yang, J. J. Li, X. Y. Lu, Z. S. Jin, L. Lu, and C. Z. Gu, Diamond Relat. Mater. **15**, 659–663 (2006).
[24]D. C. Look and R. J. Molnar, Appl. Phys. Lett. **70**, 3377–3379 (1997).
[25]G. Kresse and J. Hafner, Phys. Rev. B **47**, 558–561 (1993).
[26]Y. Wang and J. P. Perdew, Phys. Rev. B **44**, 13298–13307 (1991).
[27]H. J. Monkhorst and J. D. Pack, Phys. Rev. B **13**, 5188–5192 (1976).